arXiv:1511.08675v1 [hep-ph] 27 Nov 2015

Jet substructures of boosted polarized hadronic tops

Yoshio Kitadono* and Hsiang-nan Li†

Institute of Physics, Academia Sinica,

Taipei 11529, Taiwan, Republic of China

(Dated: November 30, 2015)

Abstract

We study jet substructures of a boosted polarized top quark, which undergoes the hadronic decay $t \to bu\bar{d}$, in the perturbative QCD framework, focusing on the energy profile and the differential energy profile. These substructures are factorized into the convolution of a hard top-quark decay kernel with a bottom-quark jet function and a W-boson jet function, where the latter is further factorized into the convolution of a hard W-boson decay kernel with two light-quark jet functions. Computing the hard kernels to leading order in QCD and including the resummation effect in the jet functions, we show that the differential jet energy profile is a useful observable for differentiating the helicity of a boosted hadronic top quark: a right-handed top jet exhibits quick descent of the differential energy profile with the inner test cone radius r, which is attributed to the V-A structure of weak interaction and the dead-cone effect associated with the W-boson jet. The above helicity differentiation may help to reveal the chiral structure of physics beyond the Standard Model at high energies.

PACS numbers: 14.65.Ha, 13.88.+e, 12.38.Cy, 13.87.-a

Keywords: Top, Helicity, Spin, Boost, Factorization, Jets, Substructure

*Electronic address: kitadono@phys.sinica.edu.tw

†Electronic address: hnli@phys.sinica.edu.tw

I. INTRODUCTION

Precise theoretical and experimental investigations of top-quark properties [1–4] are crucial not only for understanding the electroweak dynamics in the Standard Model, but also for exploring new physics beyond the Standard Model. A top quark may be produced with large boost at the Large Hadron Collider (LHC) in the future 13-14 TeV run, for example, directly through the gluon-gluon fusion, or indirectly through decays of new massive particles from Kaluza-Klein gluons [5, 6], string Regge states in the Randall-Sundrum model [7] and the supersymmetric models [8, 9], or light quark partners in the composite Higgs models [10–15]. Fixed-order calculations and soft-gluon resummations associated with the boosted top quark production have been performed in the Standard Model [16–19]. New physics beyond the Standard Model has been explored intensively in [20–27] and model independently in [28] by means of boosted top quarks.

It is known that chirality becomes equivalent to helicity for a highly boosted particle, so the helicity information of an energetic top quark may reveal the chiral structure of new physics, such as the chiral couplings of a top quark to new physics. However, the decay products of a boosted top quark may be extremely collimated to each other and form a single jet. How to differentiate a boosted top quark from ordinary QCD jets, and then to determine its helicity become a challenge at high energy colliders. Various strategies for tagging boosted top quarks were proposed in [29–36], and studied recently in [37–40]. Relevant experimental investigations have been conducted thoroughly by the ATLAS and CMS Collaborations in [41, 42].

It has been shown that the distribution in the top jet invariant mass is not sensitive to the helicity, since its peak position is basically determined by the top-quark mass [43]. Additional information on the internal structure of a top jet is then needed to distinguish its helicity. The relation between the helicity of a boosted top quark and the energy fraction distribution of a particular subjet was discussed in [44] using Monte Carlo generators. Given an algorithm for the subjet selection, different energy fraction distributions for the left- and right-handed top jets were derived. The technique of measuring the top-quark polarization in the hadronic channel was improved with the weight method in [45]. The above progress implies that jet substructures can serve as efficient observables for distinguishing the helicity of a boosted polarized top quark. Following this development, we have demonstrated in the

perturbative QCD (pQCD) framework [43] that the energy profile (jet shape) [46] of a semi-leptonic top jet is a simple and useful substructure for the helicity identification, which does not require decomposition of subjets and algorithms for subject selection as in [44], b-tagging, W-reconstruction or measurement of missing momenta.

The analysis in [43] began with the construction of a jet energy function for a polarized top quark, which undergoes the semi-leptonic decay $t \to b\ell\nu$. The lepton energy is not included, and the neutrino energy, as a missing momentum, does not contribute either. This jet energy function was factorized into the convolution of a hard top-quark decay kernel with a bottom jet energy function. The latter is well approximated by the light-quark jet energy function derived in the QCD resummation formalism [47], as the jet momentum is high enough. Evaluating the hard kernel to leading order (LO) in QCD, we obtained the dependencies of the left- and right-handed top-quark jet energy functions on the top-jet momentum, the jet cone radius R, and the radius $r \leq R$ of a test cone centered around the top jet axis. Normalizing the jet energy functions to their values at $r = R$, we predicted the energy profiles $\Psi(r)$ of the left- and right-handed top jets. It was found that the energy profile is sensitive to the helicity for the top jet momentum around 1 TeV: energy is accumulated faster within a left-handed top jet than within a right-handed one.

In this paper we will extend our formalism to the study of the energy profiles of a boosted hadronic top quark, which undergoes the $t \to bu\bar{d}$ decay, and explore the dependence of this jet substructure on the top-quark helicity. Compared to the semi-leptonic top jet, several theoretical challenges have to be overcome. The kinematics for the three-body decay $t \to bu\bar{d}$ is much more complicated, so that it is not easy to handle the angular relation among the three subjets formed by the bottom, up, and down quarks, as their energy contributions to the test cone are evaluated. With the neutrino momentum being integrated out, the semi-leptonic decay involves basically two-body kinematics. For a hadronic top jet, an additional nonperturbtive function must be introduced to absorb soft gluon exchanges among the three subjets. Even when we consider a fat bottom jet as in the semi-leptonic case [43], which absorbs soft gluons emitted by the top and bottom quarks, soft gluon exchanges remain between, for example, the up and down quarks. At last, when subjets overlap largely, their factorization becomes questionable, and the estimate of their contributions to the test cone becomes tedious in order to avoid double counting. Such a subjet merging issue does not exist in the semi-leptonic case, because only a single bottom jet appears in the final state.

Another ambiguity related to the subjet merging arises from the choices of the subjet cone radii, which complicates the organization of large logarithms involved in the jet energy profiles.

The aforementioned theoretical challenges can be overcome by the sequential factorization procedures proposed in the present work. We start with a polarized hadronic top jet, and factorize it into the convolution of a hard top-quark decay kernel with a fat W-boson jet and a fat bottom jet. The fat W-boson jet is further factorized into the convolution of a W-boson decay kernel with a fat light-quark jet and a thin light-quark jet. At each step of factorization, we just need to handle two-body kinematics of final states. The fat bottom jet absorbs the soft gluons the same as in the semi-leptonic case, namely, the bottom jet is universal for the semi-leptonic and hadronic top jets. The fat light-quark jet in the W-boson jet absorbs the rest of soft gluons emitted within the top jet, following the procedure in [48] that is applied to the absorption of soft gluons in a Higgs-boson jet. Soft gluon exchanges between the color-singlet W-boson jet and other subprocesses are expected to be suppressed in the limit of high jet energy. That is, soft gluons are handled by constructing fat subjets, instead of by introducing additional nonperturbative functions. The fat light-quark jet and the thin light-quark jet completely overlap, such that the subjet merging issue does not exist. Similarly, the fat W-boson jet and the fat bottom jet completely overlap as well. In our construction a fat subjet has radius R to absorb all soft radiations in the top jet, and a thin subjet has radius r, which is regarded as a small parameter in our formalism. We focus on the behavior of the energy profiles at small r, where the resummation technique applies. The ambiguity to define jet radii is then removed.

Including the resummation effect [47] in the quark jet functions, and evaluating the LO hard kernel under the narrow-width approximation for both the top-quark and W-boson propagators, we derive the left-handed (helicity-minus) and right-handed (helicity-plus) top jet energy functions. It is observed that the bottom jet contributes more to the energy profile of a left-handed top jet, similar to the semi-leptonic case. As explained in [43], this is a consequence attributed to the V-A structure of weak interaction. The contribution of the W-boson jet, exhibiting a more obvious dead-cone effect, starts from a larger test cone radius, and is more dominant in the energy profile of a right-handed top jet. Combining the bottom and W-boson jets, we find that the energy profile becomes insensitive to the top-quark helicity. Instead, the differential energy profile shows a more significant dependence on

the top-quark helicity: the differential energy profile of a right-handed top jet descends more quickly with the test cone radius r. Our work does not only represent an extension of pQCD to the study of jet substructures of a boosted weakly decaying massive particle, but also manifests the differential energy profile as a simple and useful observable for distinguishing the helicity of a boosted hadronic top quark.

The pQCD factorizations for the jet function and the jet energy function of a polarized hadronic top quark are formulated in Sec. II. The sensitivity of the energy profile and the differential energy profile of a hadronic top jet to the helicity is explored numerically in Sec. III. Section IV contains the conclusion. In the Appendix we explain at one-loop level that soft gluon emissions in a hadronic top jet can be absorbed into fat subjets.

II. FORMALISM

In this section we derive the factorization formulas for the jet function and the jet energy function of a highly boosted polarized hadronic top quark. The jet energy profile

$$\Psi(r) \;=\; \frac{1}{N_{J_t}} \sum_{J_t} \frac{\sum_{\theta_i<r, i\in J_t} P_{T_i}}{\sum_{\theta_i<R, i\in J_t} P_{T_i}}, \tag{1}$$

is then predicted, in which N_{J_t} is the number of top jets with the cone radius R, r is the test cone radius, P_{T_i} is the transverse momentum carried by particle i in the top jet J_t, and θ_i is the polar angle of particle i with respect to the top-jet axis.

A. Top-quark Production and Decay

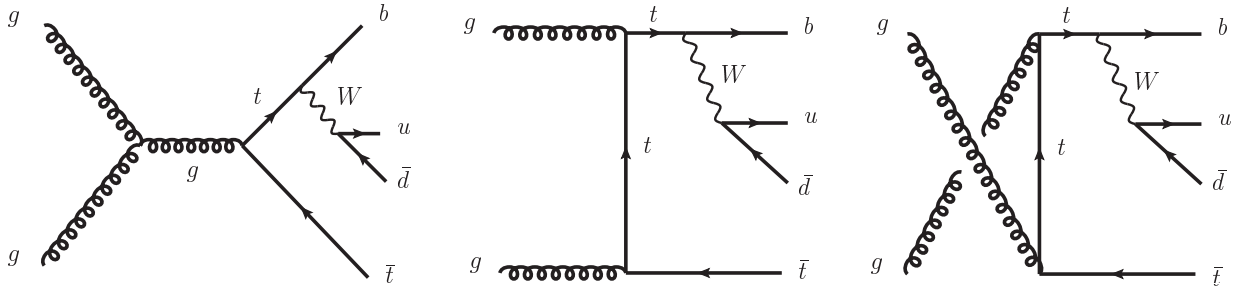

FIG. 1: LO diagrams for the top-pair production.

We consider the production process from the gluon fusion $gg \to t\bar{t}$ displayed in Fig. 1, which dominates at the LHC. The top quark then proceeds with the hadronic decay $t(k_t) \to b(k_b)u(k_u)\bar{d}(k_{\bar{d}})$, where k_i are the momenta of particle i, satisfying the conservation $k_t = k_b + k_u + k_{\bar{d}}$. Figure 1 gives the squared amplitude

$$\begin{aligned} |\overline{\mathcal{M}}|^2 \;=\; & \frac{g_s^4}{32^2} g^4 |V_{tb}|^2 |V_{ud}|^2 N_c D_t(k_t^2) D_W(k_W^2) \mathrm{tr}\left[\not{k}_u \gamma^\alpha P_L \not{k}_{\bar{d}} \gamma^\gamma P_L\right] \\ & \times \sum_{i_b, i_{\bar{t}}} \mathrm{tr}\left[(\not{k}_b + m_b)\gamma_\alpha P_L (\not{k}_t + m_t)\Gamma^{ab,\mu\nu}_{i_b i_{\bar{t}}}(\not{k}_{\bar{t}} - m_t)\bar{\Gamma}^{ab}_{i_b i_{\bar{t}},\mu\nu}(\not{k}_t + m_t)\gamma_\gamma P_L\right], \end{aligned} \tag{2}$$

in which g_s is the QCD coupling, g is the weak coupling, V_{tb} and V_{ud} are the Cabibbo-Kobayashi-Maskawa matrix element, $N_c = 3$ is the number of colors, $P_L = (1-\gamma^5)/2$ is the chiral projection matrix, and m_b is the bottom quark mass. The function

$$D_i(k_i^2) = \frac{1}{(k_i^2 - m_i^2)^2 + (m_i\Gamma_i)^2}, \tag{3}$$

comes from the top quark (W-boson) propagator as $i = t$ ($i = W$) with the top-quark (W-boson) mass m_t (m_W) and decay width Γ_t (Γ_W). The vertex function is written as

$$\Gamma^{ab,\mu\nu}_{i_b i_{\bar{t}}} = -f^{abc} t^c_{i_b i_{\bar{t}}} \frac{1}{\hat{s}} \tilde{V}_3^{\mu\nu\rho}(k_1, k_2) + i t^a_{i_b k} t^b_{k i_{\bar{t}}} \gamma^\mu \frac{\not{k}_t - \not{k}_1 + m_t}{\hat{t} - m_t^2}\gamma^\nu + i t^b_{i_b k} t^a_{k i_{\bar{t}}} \gamma^\nu \frac{\not{k}_t - \not{k}_2 + m_t}{\hat{u} - m_t^2}\gamma^\mu, \tag{4}$$

with the three-gluon vertex

$$\tilde{V}_3^{\mu\nu\rho}(k_1, k_2) \;=\; g^{\mu\nu}(k_1 - k_2)^\rho + 2k_2^\mu g^{\nu\rho} - 2k_1^\nu g^{\rho\mu}. \tag{5}$$

In the above expressions $i_{b,\bar{t}}$ label the colors of the $b, \bar{t}$ quarks, a, μ, k_1 and b, ν, k_2 denote the colors, Lorentz indices, momenta of the incoming gluons 1 and 2, respectively, and $\hat{s} = (k_1 + k_2)^2$, $\hat{t} = (k_t - k_1)^2$, and $\hat{u} = (k_t - k_2)^2$ are the kinematic invariants. Another vertex function $\bar{\Gamma}^{ab,\mu\nu}_{i_b i_{\bar{t}}}$ is the Dirac conjugate of $\Gamma^{ab,\mu\nu}_{i_b i_{\bar{t}}}$, defined as $\bar{\Gamma}^{ab,\mu\nu}_{i_b i_{\bar{t}}} \equiv \gamma^0 \left(\Gamma^{ab,\mu\nu}_{i_b i_{\bar{t}}}\right)^\dagger \gamma^0$.

The LO squared amplitude $\left|\overline{\mathcal{M}}\right|^2$ is factorized, up to power corrections of $\mathcal{O}(m_t/E_t)$, E_t being the top-quark energy, into two pieces, i.e., the production part $\left|\overline{\mathcal{M}}_{prod}\right|^2$ shown in

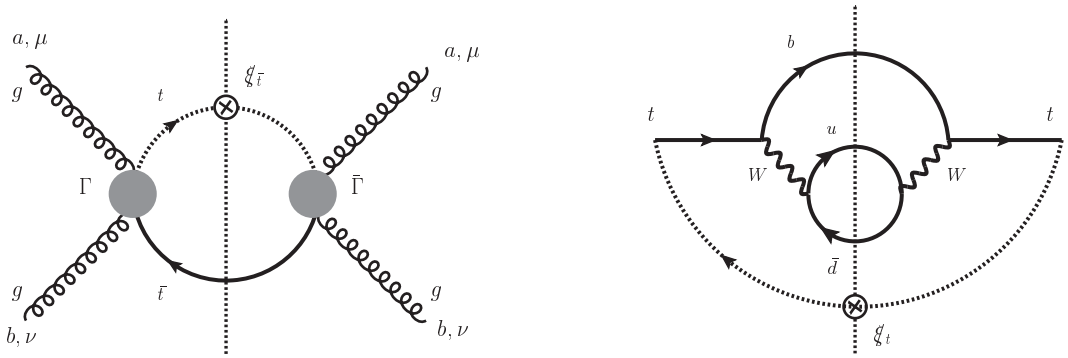

(a) (b)

FIG. 2: LO diagrams for (a) the production and (b) the hadronic decay of a top quark. The dashed lines label the fermion flows, and the symbols $\otimes$ represent the insertions of the gamma matrices $\not{\bar{\xi}}_t$ and $\not{\xi}_t$ from the Fierz identity.

Fig. 2(a) and the decay part $\left|\overline{\mathcal{M}}_{decay}\right|^2$ in Fig. 2(b):

$$\begin{aligned}
|\overline{\mathcal{M}}|^2 &= |\overline{\mathcal{M}}_{prod}|^2 |\overline{\mathcal{M}}_{decay}|^2, \\
|\overline{\mathcal{M}}_{prod}|^2 &\equiv \frac{g_s^4}{16^2}\frac{1}{4}\sum_{i_{\bar{t}},i_b} \mathrm{tr}\left[\not{\xi}_{\bar{t}}\Gamma^{ab,\mu\nu}_{i_b i_{\bar{t}}}(\not{k}_{\bar{t}} - m_t)\bar{\Gamma}^{ab}_{i_b i_{\bar{t}},\mu\nu}\right], \\
|\overline{\mathcal{M}}_{decay}|^2 &= \frac{g^4}{4}N_c|V_{tb}|^2|V_{ud}|^2 D_t(k_t^2) D_W(k_W^2) \mathrm{tr}\left[\not{k}_u\gamma^\alpha P_L \not{k}_{\bar{d}}\gamma^\gamma P_L\right] \\
&\quad \times \mathrm{tr}\left[(\not{k}_b + m_b)\gamma_\alpha P_L(\not{k}_t + m_t)\not{\xi}_t(\not{k}_t + m_t)\gamma_\gamma P_L\right]. \qquad (6)
\end{aligned}$$

The dimesionless vectors [49]

$$\xi_{\bar{t}} = \frac{1}{\sqrt{2}}(1, -\hat{n}_{\bar{t}}), \qquad \xi_t = \frac{1}{\sqrt{2}}(1, -\hat{n}_t), \qquad (7)$$

have been introduced via the Fierz transformation to break the fermion flow [43], in which the unit vectors $\hat{n}_t$ and $\hat{n}_{\bar{t}}$ are along the directions of the top-quark and anti-top-quark momenta, respectively.

B. Top Jet Function

The differential cross section for the $pp \to \bar{t}bu\bar{d}$ is then factorized into the convolution of the production cross section σ_{prod} with the top jet function J_t,

$$\frac{d\sigma(pp \to \bar{t}bu\bar{d})}{dE_{J_t}d\Omega_{J_t}dm^2_{J_t}} = \int dx_1 dx_2 \phi_g(x_1)\phi_g(x_2)\sigma_{prod}(x_1, x_2, m^2_{J_t}, E_{J_t}, \cos\theta_{J_t}) J_t(m^2_{J_t}, E_{J_t}, R), \quad (8)$$

where E_{J_t}, m_{J_t}, Ω_{J_t}, θ_{J_t}, and R are the energy, the invariant mass, the solid angle, the polar angle, and the cone radius of the top jet, respectively, and $\phi_g(x)$ is the gluon parton distribution function, x being the momentum fraction. The production cross section is written as

$$\sigma_{prod}(x_1, x_2, m^2_{J_t}, E_{J_t}, \cos\theta_{J_t}) \;=\; \frac{\pi\beta_{J_t} E_{J_t}}{4(2\pi)^3 A_t \hat{s} E_{\bar{t}}} \delta(E_1 + E_2 - E_{J_t} - E_{\bar{t}}) |\overline{\mathcal{M}}_{prod}|^2, \qquad (9)$$

with the factor $\beta_{J_t} \equiv \sqrt{1 - m^2_{J_t}/E^2_{J_t}}$, the gluonic parton energies E_1 and E_2, and the anti-top quark energy $E_{\bar{t}}$. The top jet function is defined as

$$\begin{aligned} J_t(m^2_{J_t}, E_{J_t}, R) \;=\; & A_t \int \frac{d^4k_b}{(2\pi)^3}\delta(k_b^2 - m_b^2) \int \frac{d^4k_u}{(2\pi)^3}\delta(k_u^2) \int \frac{d^4k_{\bar{d}}}{(2\pi)^3}\delta(k_{\bar{d}}^2) |\overline{\mathcal{M}}_{decay}|^2 \\ & \times\delta\left(m^2_{J_t} - (\sum k_i)^2\right) \delta\left(E_{J_t} - \sum E_i\right) \delta^{(2)}\left(\hat{n}_{J_t} - \frac{\sum \vec{k}_i}{|\sum \vec{k}_i|}\right), \end{aligned} \qquad (10)$$

in which the subscript i runs over b, u and $\bar{d}$, and the three δ-functions specify the top jet invariant mass, energy and direction in the unit vector $\hat{n}_{J_t}$. The normalization constant $A_t = (2\pi)^3/(2\sqrt{2}E^2_{J_t})$ has been chosen, such that the LO top jet function reduces to $\delta(m^2_{J_t} - m_t^2)$ without the weak decay. It is understood that the bottom, up and down quarks are restricted in the top jet cone. At higher orders, QCD radiations from the final states in the top jet, that are collimated to the top quark and in the jet cone, are grouped into J_t straightforwardly. The collinear radiations from other subprocesses, such as initial-state partons and the anti-top quark, are collected by the Wilson lines in the direction of $\xi_{J_t} = (1, -\hat{n}_{J_t})/\sqrt{2}$ [47], which are associated with the definition of J_t.

The top jet function J_t is first factorized into a hard top-quark decay kernel H_t, a fat W-boson jet function J_W with the cone radius R, and a fat bottom jet function J_b with the cone radius R, up to power corrections of $\mathcal{O}(m_{J_b}/m_{J_t})$,

$$\begin{aligned} J_t(m^2_{J_t}, E_{J_t}, R) \;=\; & \int dm^2_{J_W} dE_{J_W} d^2\hat{n}_{J_W} \int dm^2_{J_b} dE_{J_b} d^2\hat{n}_{J_b} H_t \\ & \times J_W(m^2_{J_W}, E_{J_W}, R) J_b(m^2_{J_b}, E_{J_b}, R) \\ & \times\delta\left(m^2_{J_t} - (k_{J_W} + k_{J_b})^2\right) \delta\left(E_{J_t} - E_{J_W} - E_{J_b}\right) \\ & \times\delta^{(2)}\left(\hat{n}_{J_t} - \frac{\vec{k}_{J_W} + \vec{k}_{J_b}}{|\vec{k}_{J_W} + \vec{k}_{J_b}|}\right). \end{aligned} \qquad (11)$$

The four-momentum, energy, and invariant mass of the W-boson (bottom) jet, k_{J_W}, E_{J_W}, and m_{J_W} (k_{J_b}, E_{J_b}, and m_{J_b}), respectively, are introduced according to the jet definitions

[43]. Below we will always work out the angular integration for the fat jet, obtaining

$$\int d^2\hat{n}_{J_W}\delta^{(2)}\left(\hat{n}_{J_t}-\frac{\vec{k}_{J_W}+\vec{k}_{J_b}}{|\vec{k}_{J_W}+\vec{k}_{J_b}|}\right)=\frac{|\vec{k}_{J_W}+\vec{k}_{J_b}|}{|\vec{k}_{J_W}|}=\frac{\beta_{J_t}E_{J_t}}{\beta_{J_W}E_{J_W}}. \tag{12}$$

The bottom jet will be treated as a light-quark jet here as stated before. The integration of $|\overline{\mathcal{M}}_{decay}|^2$, which contains the W-boson propagator, over the $u,\bar{d}$ kinematic variables is proportional to the sum over the W-boson polarizations, $d^{\alpha\gamma}=g^{\alpha\gamma}-k^{\alpha}_{J_W}k^{\gamma}_{J_W}/m^2_{J_W}$. Therefore, we extract the W-boson jet function according to

$$\begin{aligned}-d^{\alpha\gamma}J_W(m^2_{J_W},E_{J_W},R) &= g^2|V_{ud}|^2N_cA_W\int\frac{d^4k_u}{(2\pi)^3}\delta(k_u^2)\int\frac{d^4k_{\bar{d}}}{(2\pi)^3}\delta(k_{\bar{d}}^2)\\ &\times\mathrm{tr}\left[\not{k}_u\gamma^{\alpha}P_L\not{k}_{\bar{d}}\gamma^{\gamma}P_L\right]D_W(k^2_{J_W})\delta\left(m^2_{J_W}-(k_u+k_{\bar{d}})^2\right)\\ &\times\delta\left(E_{J_W}-E_u-E_{\bar{d}}\right)\delta^{(2)}\left(\hat{n}_{J_W}-\frac{\vec{k}_u+\vec{k}_{\bar{d}}}{|\vec{k}_u+\vec{k}_{\bar{d}}|}\right),\end{aligned} \tag{13}$$

where the normalization constant $A_W=2(2\pi)^3/E_{J_W}$ is chosen, such that the LO W-boson jet function without the weak decay reduces to $\delta(m^2_{J_W}-m^2_W)$. At higher orders, J_W absorbs the collinear radiations collimated to the W-boson and the soft radiations in the top jet. The LO hard kernel H_t is given by

$$\begin{aligned}H_t &= \frac{g^2}{8\sqrt{2}}|V_{tb}|^2\frac{A_tE_{J_t}}{A_WA_b}(1+\beta_{J_t})D_t(k^2_{J_t})(-d^{\alpha\gamma})\mathrm{tr}\left[\gamma_{\alpha}P_L(\not{k}_{J_t}+m_t)\gamma_{\gamma}P_L\bar{\not{\xi}}_{J_b}\right]\\ &+\mathcal{O}(k^2_{J_t}-m^2_t),\end{aligned} \tag{14}$$

where the normalization constant $A_b=(2\pi)^3/(2\sqrt{2}E^2_{J_b})$ is introduced through the definition of J_b [43], and the light-like vector $\bar{\xi}_{J_b}$ is along the direction of the bottom jet momentum.

Next we factorize the fat W-boson jet function into a hard W-boson decay kernel, a fat up jet function with the cone radius R, and a thin down jet function with the small cone radius r. Using the relation $g_{\alpha\gamma}d^{\alpha\gamma}=3$, we write J_W as

$$\begin{aligned}J_W(m^2_{J_W},E_{J_W},R) &= \int dm^2_{J_u}dE_{J_u}\int dm^2_{J_{\bar{d}}}dE_{J_{\bar{d}}}d^2\hat{n}_{J_{\bar{d}}}\frac{\beta_{J_W}E_{J_W}}{\beta_{J_u}E_{J_u}}H_W\\ &\times J_u(m^2_{J_u},E_{J_u},R)J_{\bar{d}}(m^2_{J_{\bar{d}}},E_{J_{\bar{d}}},r)\\ &\times\delta\left(m^2_{J_W}-(k_{J_u}+k_{J_{\bar{d}}})^2\right)\delta\left(E_{J_W}-E_{J_u}-E_{J_{\bar{d}}}\right),\end{aligned} \tag{15}$$

with the LO hard kernel

$$\begin{aligned}H_W &= g^2|V_{ud}|^2N_c\frac{A_W}{A_uA_{\bar{d}}}\frac{-g_{\alpha\gamma}}{3}\left[\bar{\not{\xi}}_{J_u}\gamma^{\alpha}P_L\bar{\not{\xi}}_{J_{\bar{d}}}\gamma^{\gamma}P_L\right]D_W(k^2_{J_W}),\\ &= \frac{g^2}{12\pi^3}|V_{ud}|^2N_c\frac{E^2_{J_u}E^2_{J_{\bar{d}}}}{E_{J_W}}[1-\cos(\theta_{J_u}+\theta_{J_{\bar{d}}})]D_W(k^2_{J_W}).\end{aligned} \tag{16}$$

In the above expressions k_{J_u}, E_{J_u}, θ_{J_u}, and m_{J_u} ($k_{J_{\bar{d}}}$, $E_{J_{\bar{d}}}$, $\theta_{J_{\bar{d}}}$, and $m_{J_{\bar{d}}}$) are the four-momentum, energy, angle, and invariant mass of the up-quark (down-quark) jet, respectively. The constant $A_u = (2\pi)^3/(2\sqrt{2}E_{J_u}^2)$ ($A_{\bar{d}} = (2\pi)^3/(2\sqrt{2}E_{J_d}^2)$) is introduced to normalize the up (down) jet function to a δ-function at LO in α_s [47]. To factorize the up and down jet functions from the W-boson jet function, we also need to introduce the light-like vectors $\bar{\xi}_{J_u}$ and $\bar{\xi}_{J_{\bar{d}}}$ along the directions of the up-jet and down-jet momenta, respectively, as a consequence of the Fierz transformation [47]. Their inner product gives $\bar{\xi}_{J_u} \cdot \bar{\xi}_{J_{\bar{d}}} = [1 - \cos(\theta_{J_u} + \theta_{J_{\bar{d}}})]/2$ in the second line of Eq. (16).

At last, to discuss the dependence on the top-quark helicity, we insert the top-spin projectors

$$w_{s_t} = \frac{1}{2}(\mathbf{1} + \gamma^5 \not{s}_t), \qquad \bar{w}_{s_t} = \frac{1}{2}(\mathbf{1} - \gamma^5 \not{s}_t), \tag{17}$$

under which the unpolarized top jet function is decomposed into $J_t = J_t^{s_t} + J_t^{\bar{s}_t}$. The corresponding hard top-quark decay kernel for $J_t^{s_t}$ is given by

$$\begin{aligned} H_t^{s_t} &= \frac{g^2}{8\sqrt{2}}|V_{tb}|^2 \frac{A_t E_{J_t}}{A_W A_b}(1+\beta_{J_t}) D_t(k_{J_t}^2)(-d^{\alpha\gamma}) \mathrm{tr}\left[\gamma_\alpha P_L(\not{k}_{J_t} + m_t) w_{s_t} \gamma_\gamma P_L \not{\bar{\xi}}_{J_b}\right], \\ &= \frac{g^2}{16(2\pi)^3}|V_{tb}|^2 \frac{E_{J_W} E_{J_b}}{E_{J_t}}(1+\beta_{J_t}) D_t(k_{J_t}^2) \\ &\quad \times \left[\left(\frac{m_{J_t}^2}{m_{J_W}^2} + 2\right)\left(\frac{m_{J_t}^2 - m_{J_W}^2}{2}\right) + \left(\frac{m_{J_t}^2}{m_{J_W}^2} - 2\right) m_t E_{J_b}\left(s_t^0 - |\vec{s}_t|\cos\theta_{J_b}\right)\right], \end{aligned} \tag{18}$$

and $H_t^{\bar{s}_t}$ for $J_t^{\bar{s}_t}$ is similar, but with w_{s_t} being replaced by $\bar{w}_{s_t}$. The W-boson jet function and the bottom jet function in the factorization formulas for $J_t^{s_t}$ and $J_t^{\bar{s}_t}$ are the same as for the unpolarized top jet function. The absolute value of the top spin in the boosted frame is set to $|\vec{s}_t| = 1/\sqrt{1-\beta_{J_t}^2}$, and the zeroth component is then given by $s_t^0 = \beta_{J_t}|\vec{s}_t|$.

C. Top Jet Energy Function

Following the reasoning in [47], we construct the polarized top jet energy function J_t^{E,s_t} by accumulating the energy of final-state particles in the test cone of radius r. It is straight-

forward to derive the factorization formula

$$
\begin{aligned}
J_t^{E,s_t}(m_{J_t}^2, E_{J_t}, R, r) \;=\; & \int dm_{J_W}^2 dE_{J_W} \int dm_{J_b}^2 dE_{J_b} d^2\hat{n}_{J_b} \frac{\beta_{J_t} E_{J_t}}{\beta_{J_W} E_{J_W}} H_t^{s_t} \\
& \times \left[J_b^E(m_{J_b}^2, E_{J_b}, R, r) J_W(m_{J_W}^2, E_{J_W}, R) \Theta(ar - \theta_{J_b}) \right. \\
& \left. + J_W^E(m_{J_W}^2, E_{J_W}, R, r) J_b(m_{J_b}^2, E_{J_b}, R) \Theta(ar - \theta_{J_W}) \right] \\
& \times \delta\left(m_{J_t}^2 - (k_{J_W} + k_{J_b})^2\right) \delta\left(E_{J_t} - E_{J_W} - E_{J_b}\right), \qquad (19)
\end{aligned}
$$

where $a \sim \mathcal{O}(1)$ is a geometric factor to be specified below. The bottom (W-boson) jet energy function $J_{b(W)}^E$ absorbs QCD radiations, which are associated with the bottom (W-boson) jet and go into the test cone. That is, the first (second) term describes the contribution to the top jet energy profile from the bottom (W-boson) jet. The Θ function requires the polar angle of a subjet to be smaller than ar, if it contributes to the energy profile.

It should be pointed out that the contribution to the energy profile from the hard gluons has been neglected in Eq. (19), which appears at next-to-leading order in QCD. To be consistent with this accuracy, the parameter a is set to $a = 2$ to minimize the contribution from hard gluons [48]. In the present work we will approximate the fat bottom jet by a thin bottom jet of cone radius r, for which the simplification $J_b^E(m_{J_b}^2, E_{J_b}, r, r) = E_{J_b} J_b(m_{J_b}^2, E_{J_b}, r)$ holds. The overestimate of the top jet energy profile due to this approximation can be compensated by choosing a value of $a < 2$. We have confirmed that $a = 1.7$ is the best choice, which reproduces the fat bottom jet contribution in the considered kinematic region. In other words, the choice $a = 1.7$ includes the resummation effect in the fat jet contribution. Neglecting the small bottom jet invariant mass m_{J_b} in the hard kernel $H_t^{s_t}$ and in the δ-functions, we can integrate out the m_{J_b} dependence, and have $\int dm_{J_b}^2 J_b(m_{J_b}^2, E_{J_b}, r) = 1 + \mathcal{O}(\alpha_s)$.

The narrow-width approximation is then applied to both the W-boson and top-quark propagators $D_{i=t,W}$,

$$
D_i(m_{J_i}^2) \approx \frac{\pi}{m_i \Gamma_i} \delta(m_{J_i}^2 - m_i^2), \qquad (20)
$$

so that the integration over the W-boson jet invariant mass $m_{J_W}^2$ in Eq. (19) can be carried out trivially, with all $m_{J_W}^2$ being replaced by the W-boson mass m_W^2. The polarized top jet

energy function is then simplified into

$$
\begin{aligned}
J_t^{E,s_t}(m^2_{J_t}, E_{J_t}, R, r) \;=\; & \int dE_{J_W} \int dE_{J_b} d^2\hat{n}_{J_b} \frac{\beta_{J_t}}{\beta_W} R^2 E_{J_t} E_{J_W} H_t^{s_t} \\
& \times \left[E_{J_b} \bar{J}_W(N=1, E_{J_W}, R) \Theta(ar - \theta_{J_b}) \right. \\
& \quad \left. + \bar{J}_W^E(N=1, E_{J_W}, R, r) \Theta(ar - \theta_{J_W}) \right] \\
& \times \delta\left(m^2_{J_t} - (k_{J_W} + k_{J_b})^2\right) \delta\left(E_{J_t} - E_{J_W} - E_{J_b}\right), \qquad (21)
\end{aligned}
$$

with the factor $\beta_W = \sqrt{1 - m_W^2/E_{J_W}^2}$, and the first moments of the W-boson jet function and energy function

$$
\begin{aligned}
\int \frac{dm^2_{J_W}}{(RE_{J_W})^2} J_W(m^2_{J_W}, E_{J_W}, R) \;&=\; \bar{J}_W(N=1, E_{J_W}, R), \\
\int \frac{dm^2_{J_W}}{(RE_{J_W})^2} J_W^E(m^2_{J_W}, E_{J_W}, R, r) \;&=\; \bar{J}_W^E(N=1, E_{J_W}, R, r), \qquad (22)
\end{aligned}
$$

respectively.

As in [43], we boost the top quark such that $H_t^{s_t}$ in Eq. (18) corresponds to the top-quark decay kernel of helicity plus $h = +$ and $H_t^{\bar{s}_t}$ corresponds to helicity minus $h = -$. The narrow-width approximation for the top-quark propagator allows us to compute the first moment of the top jet energy function $J_t^{E,h=\pm}$ easily,

$$
\begin{aligned}
\bar{J}_t^{E,h=\pm}(1, E_{J_t}, R, r) \;=\; & \frac{g^2}{64\pi} |V_{tb}|^2 (1+\beta_t) \beta_t \frac{E_{J_t}^2}{m_t \Gamma_t} \int dz_{J_b} d\cos\theta_{J_b} z_{J_b} (1 - z_{J_b})^2 \\
& \times \left[\left(\frac{m_t^2}{m_W^2} + 2 \right) \left(\frac{m_t^2 - m_W^2}{2} \right) \right. \\
& \quad \left. \pm \left(\frac{m_t^2}{m_W^2} - 2 \right) z_{J_b} m_t E_{J_t} \left(s_t^0 - |\vec{s}_t| \cos\theta_{J_b} \right) \right], \\
& \times \frac{1}{\beta_W} \left[z_{J_b} E_{J_t} \bar{J}_W(1, (1-z_{J_b}) E_{J_t}, R) \Theta(ar - \theta_{J_b}) \right. \\
& \quad \left. + \bar{J}_W^E(1, (1-z_{J_b}) E_{J_t}, R, r) \Theta(ar - \theta_{J_W}) \right] \\
& \times \delta\left(m_t^2 - m_W^2 - 2 z_{J_b} (1 - z_{J_b}) E_{J_t}^2 [1 - \beta_W \cos(\theta_{J_W} + \theta_{J_b})] \right), \qquad (23)
\end{aligned}
$$

with the factor $\beta_t = \sqrt{1 - m_t^2/E_{J_t}^2}$ and the energy fraction $z_{J_b} = E_{J_b}/E_{J_t}$ for the bottom jet.

The factorization formula for the W-boson jet energy function is written as

$$\begin{aligned} J_W^E(m_{J_W}^2, E_{J_W}, R, r) &= \int dm_{J_u}^2 dE_{J_u} \int dm_{J_{\bar{d}}}^2 dE_{J_{\bar{d}}} d^2\hat{n}_{J_{\bar{d}}} \frac{\beta_{J_W} E_{J_W}}{\beta_{J_u} E_{J_u}} H_W \\ &\times \Big[J_u^E(m_{J_u}^2, E_{J_u}, R, r) J_{\bar{d}}(m_{J_{\bar{d}}}^2, E_{J_{\bar{d}}}, r) \Theta(ar - \theta_{J_u}) \\ &+ J_u(m_{J_u}^2, E_{J_u}, R) J_{\bar{d}}^E(m_{J_{\bar{d}}}^2, E_{J_{\bar{d}}}, r, r) \Theta(ar - \theta_{J_{\bar{d}}}) \Big] \\ &\times \delta\left(m_{J_W}^2 - (k_{J_u} + k_{J_{\bar{d}}})^2\right) \delta\left(E_{J_W} - E_{J_u} - E_{J_{\bar{d}}}\right), \qquad (24) \\ &\approx 2 \int dm_{J_u}^2 dE_{J_u} \int dm_{J_{\bar{d}}}^2 dE_{J_{\bar{d}}} d^2\hat{n}_{J_{\bar{d}}} \frac{\beta_{J_W} E_{J_W}}{\beta_{J_u} E_{J_u}} H_W \\ &\times J_u(m_{J_u}^2, E_{J_u}, R) J_{\bar{d}}^E(m_{J_{\bar{d}}}^2, E_{J_{\bar{d}}}, r, r) \Theta(ar - \theta_{J_{\bar{d}}}) \\ &\times \delta\left(m_{J_W}^2 - (k_{J_u} + k_{J_{\bar{d}}})^2\right) \delta\left(E_{J_W} - E_{J_u} - E_{J_{\bar{d}}}\right), \qquad (25) \end{aligned}$$

where the meaning of each factor can be understood in a similar way. Inputting the jet functions and the jet energy functions from the resummation formalism [47], one can compute $J_W^E(m_{J_W}^2, E_{J_W}, R, r)$ in principle. Here we have approximated the fat jet contribution to the W-boson jet energy function by the thin jet contribution again with the parameter $a = 1.7$, as deriving Eq. (25) from Eq. (24) .

To get analytical expressions for the W-boson jet function and energy function, we simplify the thin down jet energy function into $J_{\bar{d}}^E(m_{J_{\bar{d}}}^2, E_{J_{\bar{d}}}, r, r) = E_{J_{\bar{d}}} J_{\bar{d}}(m_{J_{\bar{d}}}^2, E_{J_{\bar{d}}}, r)$, and approximate the up jet function by a δ-function [48] and β_{J_u} by $\beta_{J_u} \approx 1$ in Eq. (25). The conservation of the momenta perpendicular to the W-boson jet axis gives the relation $E_{J_u}\theta_{J_u} = E_{J_{\bar{d}}}\theta_{J_{\bar{d}}}$ in the small angle limit, i.e., in the small m_W/E_{J_W} limit. The narrow-width approximation then determines the relation between the down jet energy fraction $y_{J_{\bar{d}}} = E_{J_{\bar{d}}}/E_{J_W}$ and the polar angle $\theta_{J_{\bar{d}}}$,

$$\theta_{J_{\bar{d}}}^2 \approx \frac{E_{J_u} m_W^2}{E_{J_{\bar{d}}} E_{J_W}^2}. \qquad (26)$$

The W-boson jet function and energy function reduce to

$$\bar{J}_W(N = 1, E_{J_W}, R) = \frac{g^2}{4\pi} \frac{\beta_W m_W}{R^2 E_{J_W}^2 \Gamma_W} |V_{ud}|^2 \int_{y^m}^{y^M} dy_{J_{\bar{d}}} (1 - y_{J_{\bar{d}}}), \qquad (27)$$

$$\bar{J}_W^E(N = 1, E_{J_W}, R, r) = \frac{g^2}{2\pi} \frac{\beta_W m_W}{R^2 E_{J_W} \Gamma_W} |V_{ud}|^2 \int_{y_E^m}^{y_E^M} dy_{J_{\bar{d}}} y_{J_{\bar{d}}} (1 - y_{J_{\bar{d}}}), \qquad (28)$$

where $N_c = 3$ has been adopted in Eq. (16).

The requirement that both light-quark jets are inside the W-boson jet cone give the constraints $\theta_{J_{\bar{d}}}^2 = (1 - y_{J_{\bar{d}}})\hat{m}_W^2 / y_{J_{\bar{d}}} < R^2$ and $\theta_{J_u}^2 = y_{J_{\bar{d}}} \hat{m}_W^2 / (1 - y_{J_{\bar{d}}}) < R^2$ for Eq. (15) with

$\hat{m}_W = m_W/E_{J_W}$. They lead to the integration range $y^m < y_{J_{\bar{d}}} < y^M$ in Eq. (27) with the bounds

$$y^m = \frac{\hat{m}_W^2}{R^2 + \hat{m}_W^2}, \qquad y^M = \frac{R^2}{R^2 + \hat{m}_W^2}. \tag{29}$$

The above inequality implies that the contribution from the region of $E_{J_W} \to m_W$ is suppressed by phase space. The similar requirement together with the Θ function in Eq. (25) give $(1 - y_{J_{\bar{d}}})\hat{m}_W^2/y_{J_{\bar{d}}} < \min(R^2, a^2 r^2)$ and $y_{J_{\bar{d}}}\hat{m}_W^2/(1 - y_{J_{\bar{d}}}) < R^2$, which set the bounds in Eq. (28),

$$y_E^m = \frac{\hat{m}_W^2}{\hat{m}_W^2 + \min(R^2, a^2 r^2)}, \qquad y_E^M = \frac{R^2}{R^2 + \hat{m}_W^2}. \tag{30}$$

The δ-function in Eq. (23) leads, in the small angle limit, i.e., in the expansion of m_W/E_{J_W} and m_t/E_{J_t}, to

$$\begin{aligned} \theta_{J_b}^2 &\approx \frac{E_{J_W} m_t^2 - E_{J_t} m_W^2}{E_{J_b} E_{J_t}^2}, \\ \theta_{J_W}^2 &\approx \frac{E_{J_b}(E_{J_W} m_t^2 - E_{J_t} m_W^2)}{E_{J_W}^2 E_{J_t}^2}. \end{aligned} \tag{31}$$

Equation (23) is then simplified into

$$\begin{aligned} \bar{J}_t^{E,h=\pm}(1, E_{J_t}, R, r) \;=\; & \frac{g^4}{256\pi^2} \frac{|V_{tb}|^2 |V_{ud}|^2 m_W}{R^2 \Gamma_t \Gamma_W} \int dz_{J_b} (1 - z_{J_b}) \\ & \times \left[\left(\frac{m_t^2}{m_W^2} + 2 \right) \left(\frac{m_t^2 - m_W^2}{2 m_t E_{J_t}} \right) \pm z_{J_b} \left(\frac{m_t^2}{m_W^2} - 2 \right) \left(s_t^0 - |\vec{s}_t| \cos\theta_{J_b} \right) \right], \\ & \times \left[z_{J_b} \int_{y^m}^{y^M} dy_{J_{\bar{d}}} (1 - y_{J_{\bar{d}}}) \Theta(ar - \theta_{J_b}) \right. \\ & \left. + 2(1 - z_{J_b}) \int_{y_E^m}^{y_E^M} dy_{J_{\bar{d}}} y_{J_{\bar{d}}} (1 - y_{J_{\bar{d}}}) \Theta(ar - \theta_{J_W}) \right]. \end{aligned} \tag{32}$$

The two step functions $\Theta(ar - \theta_{J_b})$ and $\Theta(ar - \theta_{J_W})$ constrain the integration variable z_{J_b} for the bottom jet and W-boson jet contributions, respectively. Together with Eq. (29), which requires $\hat{m}_W < R$, we derive the bounds $z_1^m < z_{J_b} < z_1^M$ for the former with

$$z_1^m = \frac{\tilde{m}_t^2 - \tilde{m}_W^2}{\tilde{m}_t^2 + \min(R^2, a^2 r^2)}, \qquad z_1^M = 1 - \frac{\tilde{m}_W}{R}, \tag{33}$$

and $\tilde{m}_t = m_t/E_{J_t}$ and $\tilde{m}_W = m_W/E_{J_t}$. It is trivial to verify that the above lower and upper bounds always obey their inequality for arbitrary r, $R \sim \mathcal{O}(1)$ and $E_{J_t} \sim \mathcal{O}(1)$ TeV.

That is, there is no significant dead-cone effect for the bottom jet contribution. Besides, the W-boson jet always remains inside the top jet cone of radius R in the above range of z_{J_b}.

As to the W-boson jet contribution, we have $z_{J_b} < z_2^M$ for the lower and upper bounds in Eq. (30) to hold their inequality. The requirement that the bottom jet is inside the top jet cone sets $z_{J_b} > z_2^m$. The combination of the above two constraints,$z_2^m < z_{J_b} < z_2^M$, with

$$z_2^m = \frac{\tilde{m}_t^2 - \tilde{m}_W^2}{R^2 + \tilde{m}_t^2}, \qquad z_2^M = 1 - \frac{\tilde{m}_W}{[R^2 \min(R^2, a^2 r^2)]^{1/4}}, \tag{34}$$

implies

$$ar > \left(\frac{R^2 + \tilde{m}_t^2}{R^2 + \tilde{m}_W^2}\right)^2 \frac{\tilde{m}_W^2}{R}, \tag{35}$$

namely, a more significant dead-cone effect for the W-boson jet contribution. For $ar < (\tilde{m}_t^2 - \tilde{m}_W^2)/(2\tilde{m}_W)$, there exist additional constraints from the W-boson jet to be inside the test cone or the top jet cone, $z_{J_b} < z_2^{m\prime}$ or $z_{J_b} > z_2^{M\prime}$, with

$$\begin{aligned} z_2^{m\prime} &= \frac{2\min(R^2, a^2 r^2) + \tilde{m}_t^2 - \tilde{m}_W^2 - \sqrt{(\tilde{m}_t^2 - \tilde{m}_W^2)^2 - 4\min(R^2, a^2 r^2)\tilde{m}_W^2}}{2(R^2 + \tilde{m}_t^2)}, \\ z_2^{M\prime} &= \frac{2\min(R^2, a^2 r^2) + \tilde{m}_t^2 - \tilde{m}_W^2 + \sqrt{(\tilde{m}_t^2 - \tilde{m}_W^2)^2 - 4\min(R^2, a^2 r^2)\tilde{m}_W^2}}{2(R^2 + \tilde{m}_t^2)}. \end{aligned} \tag{36}$$

The allowed region of z_{J_b} for the W-boson jet contribution in Eq. (32) then comes from the overlap of the above range with $z_2^m < z_{J_b} < z_2^M$. Note that the bounds in Eq. (36) are effective only at small $r \sim 0.1$ for the top jet energy $E_{J_t} > 500$ GeV.

III. NUMERICAL ANALYSIS

In this section we evaluate the jet energy profiles of a boosted polarized hadronic top quark derived in Eq. (32). In the moment space the convolution in the momentum fractions in Eq. (8) becomes a product, such that the top jet energy profile $\Psi(E_{J_t}, R, r)$ can be simply calculated as the ratio

$$\Psi^{\pm}(E_{J_t}, R, r) = \frac{\bar{J}_t^{E,h=\pm}(1, E_{J_t}, R, r)}{\bar{J}_t^{E,h=\pm}(1, E_{J_t}, R, R)}, \tag{37}$$

in which the production part has been canceled between the numerator and the denominator. We take the parameters $m_t = 173.5$ GeV, $m_W = 80.39$ GeV, $\Gamma_W = 2.09$ GeV, $|V_{tb}| = 1.0$, and $R = 0.7$ for the numerical analysis below.

We display the energy profiles of the top jet, which come only from the bottom-jet contribution, in Figs. 3(a), 3(b) and, 3(c) for the top jet energy $E_{J_t} = 500$ GeV, 1 TeV and 2 TeV, respectively. It is found that the bottom jet contributes more to the energy profile of a helicity-minus top quark, similar to the semi-leptonic top case [43]. The difference of the energy profiles between two opposite helicities decreases, when the top jet energy increases as expected [43]. The top jet energy profiles, which contain only the W-boson jet contribution, are shown in Figs. 4(a), 4(b), and 4(c) for $E_{J_t} = 500$ GeV, 1 TeV and 2 TeV, respectively. Contrary to the bottom jet, the W-boson jet contributes more to the energy profile of a right-handed top quark. It has been explained in [43] that the above results are attributed to the feature of the $V - A$ weak interaction. Moreover, the W-boson contribution exhibits a more obvious dead-cone effect as highlighted by the sharp increase of the curves with the test cone radius r in Fig. 4(a).

The jet energy profiles of a boosted hadronic top quark including the contributions from both the bottom and W-boson jets are exhibited in Figs. 5(a), 5(b), and 5(c) for $E_{J_t} = 500$ GeV, 1 TeV and 2 TeV, respectively. Since the bottom jet contributes more to the left-handed top, and the W-boson jet contributes more to the right-handed top, it turns out that their contributions compensate each other, and there is tiny dependence of the energy profiles on the top-quark helicity. On the other hand, the energy profile of a top jet differs dramatically from that of a QCD jet [47]: the former has a lower $\Psi(r)$ at small r due to the dead-cone effect, but increases faster with r once the energetic subjets from the weak decay of the heavy parent particle start to contribute. A careful look of Fig. 5 reveals a richer structure of the energy profile in the hadronic top case than in the semi-leptonic top case, which arises form the interplay between the bottom-quark and W-boson contributions with different behaviors in r. This unique feature is attributed to the involved cascade weak hadronic decays of massive particles.

To see the slope change in the energy profile more clearly, we consider the differential jet

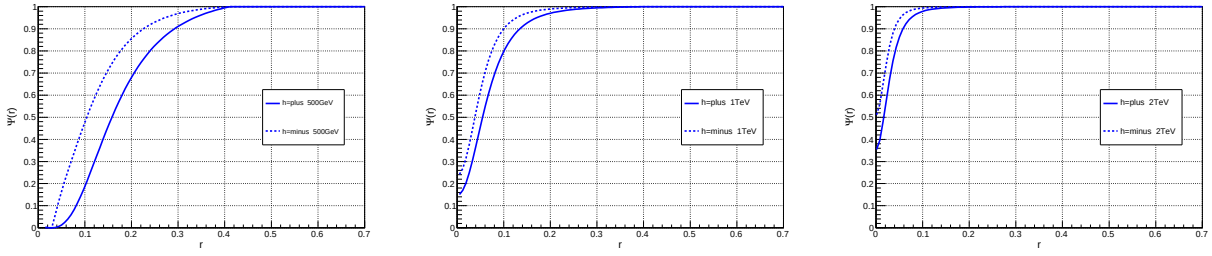

(a) (b) (c)

FIG. 3: Bottom jet contributions to the top jet energy profiles for (a) $E_{J_t} = 500$ GeV, (b) $E_{J_t} = 1$ TeV, and (c) $E_{J_t} = 2$ TeV. The top jet radius is set to $R = 0.7$.

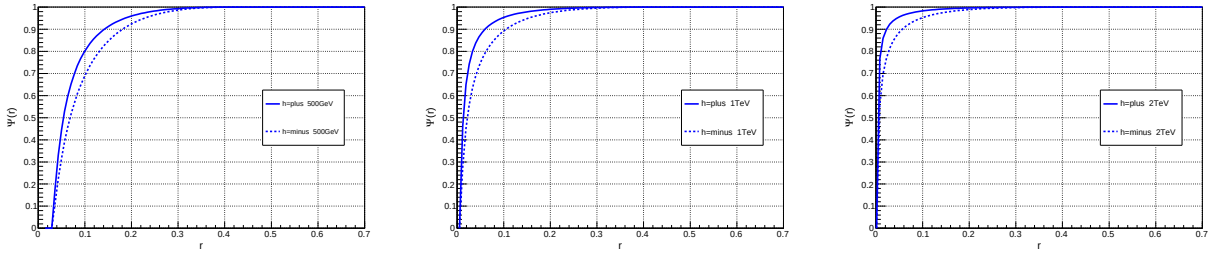

(a) (b) (c)

FIG. 4: W-boson jet contributions to the top jet energy profiles for (a) $E_{J_t} = 500$ GeV, (b) $E_{J_t} = 1$ TeV, and (c) $E_{J_t} = 2$ TeV. The top jet radius is set to $R = 0.7$.

energy profile $\rho(r)$ defined by

$$\rho(E_{J_t}, R, r) \equiv \frac{d}{dr}\Psi(E_{J_t}, R, r), \tag{38}$$

whose results are displayed in Figs. 6(a), 6(b), and 6(c) for the top jet energy $E_{J_t} = 500$

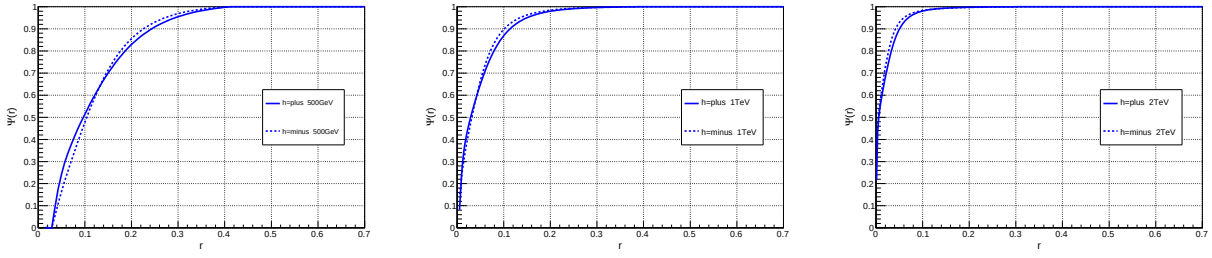

(a) (b) (c)

FIG. 5: Energy profiles of hadronic top jets for (a) $E_{J_t} = 500$ GeV, (b) $E_{J_t} = 1$ TeV, and (c) $E_{J_t} = 2$ TeV. The top jet radius is set to $R = 0.7$.

GeV, 1 TeV, and 2 TeV, respectively. The differential jet energy profiles decrease with r, similar to what was observed for QCD jets, but do not follow smooth curves. The differential jet energy profiles of a right-handed top jet start with larger values, exhibit more significant drops with r, and go below those of a left-handed top jet. This feature persists even for the top jet energy as high as 2 TeV, so the differential jet energy profile can serve as a useful observable for the helicity identification of a highly boosted hadronic top quark. The curves from the opposite top helicities become indistinguishable as $r > 0.2$ ($r > 0.08$, $r > 0.03$) for $E_{J_t} = 500$ GeV (1 TeV, 2 TeV). Since the difference of the jet energy profiles moves toward small r, its measurement will be challenging when the top jet energy increases.

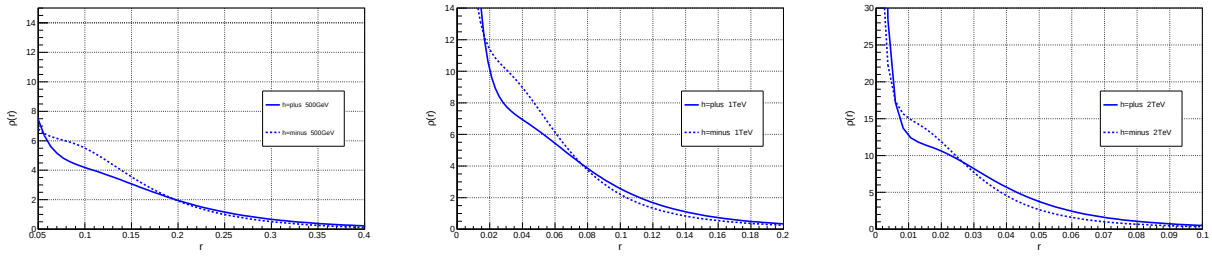

(a) (b) (c)

FIG. 6: Differential energy profiles of hadronic top jets for (a) $E_{J_t} = 500$ GeV, (b) $E_{J_t} = 1$ TeV, and (c) $E_{J_t} = 2$ TeV. The top jet radius is set to $R = 0.7$.

IV. CONCLUSION

In this paper we have studied jet substructures of a boosted polarized top quark, which undergoes the hadronic decay $t \to bu\bar{d}$, in the pQCD framework, focusing on the energy profile and the differential energy profile. These substructures were factorized into the convolution of a hard top-quark decay kernel with a fat bottom jet and a fat W-boson jet, where the latter is further factorized into the convolution of a hard W-boson decay kernel with a fat light-quark jet and a thin light-quark jet. In this sequential factorization, the complicated three-body final-state kinematics was simplified into two-body one, the soft gluon exchanges among the subjets were absorbed into the fat subjets, and the jet merging ambiguity was avoided. The pQCD analysis of the substructures of a hadronic top jet then

becomes feasible, and the formalism presented in this work contributes to the extraction of the top-quark property from experimental observations.

Computing the heavy-particle decay kernels to LO in QCD and including the resummation effect in the jet functions, we have found that the energy profile is not sensitive to the top-quark helicity because of the compensation between the bottom-quark and W-boson contributions, in which the former (latter) is more dominant in the left-handed (right-handed) top jet. Instead, the differential energy profile exhibits a richer structure due to the interplay between the bottom-quark and W-boson contributions, namely, to the involved cascade weak hadronic decays of massive particles, which also differs dramatically from that of a QCD jet. The differential energy profile of a right-handed top jet starts with a larger value, exhibits a more significant drop with r, and becomes lower than that of a left-handed top jet, a feature which persists even for the top jet energy as high as 2 TeV. However, this drop is located at very small r, whose observation will be challenging. It is worthwhile to measure such a feature, which will help to distinguish the helicity of a highly boosted hadronic top quark, and reveal the chiral structure of physics beyond the Standard Model.

Acknowledgments

We thank B. Tweedie and C.P. Yuan for helpful discussions. This work was supported in part by the Ministry of Science and Technology of R.O.C. under Grant No. NSC-104-2112-M-001-037-MY3.

Appendix A: SOFT-GLUON CONTRIBUTION AT ONE LOOP

In this appendix we calculate soft-gluon corrections to a hadronic top jet at one loop, and demonstrate that their contributions can be absorbed into the fat subjets in the factorization of the hadronic top jet. First, a soft gluon emitted by or attaching to the hard top-quark decay kernel leads to power-suppressed correction, which will be neglected here. Soft gluons emitted by other lines (the light quarks and the Wilson links associated with the top jet definition) can be factorized through the standard eikonal approximation into a nonperturbative soft function $S(\omega)$, ω being proportional to the soft gluon energy [48]. The soft function from virtual and real gluons exchanged between two pairs of eikonal lines in

the directions $\bar{\xi}_1$ and $\bar{\xi}_2$ within the top jet cone is given, at one loop, by [48]

$$S^{(1)} = \frac{\alpha_s C_F}{\pi (R E_{J_t})^2} \ln \frac{\bar{\xi}_1^2 \bar{\xi}_2^2}{4(\bar{\xi}_1 \cdot \bar{\xi}_2)^2} \left(\frac{1}{\epsilon} + \ln \frac{4\pi \mu_f^2 \bar{N}^2}{R^4 E_{J_t}^2 e^{\gamma_E}} \right), \tag{A1}$$

where μ_f is a factorization scale, the color factor $C_F = 4/3$ and the moment $\bar{N} \equiv N \exp(\gamma_E)$, with γ_E being the Euler constant. As $\bar{\xi}_i$ represents the direction of light subjet i, the invariant $\bar{\xi}_i^2$ implies that $S^{(1)}$ contains the collinear dynamics which has been absorbed into the light subjet function J_i. Collinear subtraction from the soft function is thus necessary for avoiding double counting of collinear dynamics.

In the semi-leptonic top jet soft gluons are exchanged only between the bottom quark and the Wilson line along the direction ξ_t that appears in the top-jet definition at leading power. Therefore, the soft correction $S_{b\xi}^{(1)}$ is obtained by the substitutions $\bar{\xi}_1 \to \bar{\xi}_{J_b}$ and $\bar{\xi}_2 \to \xi_{J_t}$ in Eq. (A1). The bottom jet in the semi-leptonic top jet is chosen as a fat jet of cone radius R [43]. The collinear subtraction term to be deducted from Eq. (A1) is written as

$$S_b^{(1)} = \frac{\alpha_s C_F}{\pi (R E_{J_t})^2} \ln \frac{\bar{\xi}_{J_b}^2 \xi_{J_b}^2}{4(\bar{\xi}_{J_b} \cdot \xi_{J_b})^2} \left(\frac{1}{\epsilon} + \ln \frac{4\pi \mu_f^2 \bar{N}^2}{R^4 E_{J_t}^2 e^{\gamma_E}} \right), \tag{A2}$$

where ξ_{J_b} denotes the direction of the Wilson line in the bottom jet definition. Because ξ_{J_t} may not be close to the light cone in the top jet construction, no collinear subtraction associated with this vector is needed.

The combination of Eqs. (A1) and (A2) yields

$$S_{b\xi}^{(1)} - S_b^{(1)} = \frac{\alpha_s C_F}{\pi (R E_{J_t})^2} \ln \frac{R^2 \xi_{J_t}^2}{4(\bar{\xi}_{J_b} \cdot \xi_{J_t})^2} \left(\frac{1}{\epsilon} + \ln \frac{4\pi \mu_f^2 \bar{N}^2}{R^4 E_{J_t}^2 e^{\gamma_E}} \right), \tag{A3}$$

in which we have further imposed the condition $4(\bar{\xi}_{J_b} \cdot \xi_{J_b})^2 / \xi_{J_b}^2 = R^2$ for defining a quark jet in the resummation formalism [47]. With the similar condition for the top jet, $4(\bar{\xi}_{J_t} \cdot \xi_{J_t})^2 / \xi_{J_t}^2 = R^2$, it is trivial to show that the logarithmic coefficient $\ln\{R^2 \xi_{J_t}^2 / [4(\bar{\xi}_{J_b} \cdot \xi_{J_t})^2]\}$ is proportional to the polar angle θ_{J_b} of the bottom jet. Equation (31) then implies that Eq. (A3) represents a power-suppressed correction, and is negligible. That is, soft gluons have been absorbed into the fat bottom jet in the semi-leptonic top jet, and the remaining soft corrections are of higher powers. In the hadronic top jet, the soft gluons exchanged between the bottom quark and the Wilson line in the direction ξ_{J_t} within the top cone of radius R is the same as $S_{b\xi}^{(1)}$. The bottom jet is chosen as a fat one with the cone radius R in

this case, so the collinear subtraction term is also the same as in Eq. (A3). The subtracted soft correction $S^{(1)}_{b\xi} - S^{(1)}_b$ is thus negligible.

It has been demonstrated that the soft gluons exchanged between the fat subjet and the thin subjet in the W-boson jet can be absorbed into the fat subjet [48]. Here we quoted the one-loop soft correction and the collinear subtraction terms with the up jet being a fat subjet, and the down jet being a thin subjet,

$$\begin{aligned}
S^{(1)}_{ud} &= \frac{\alpha_s C_F}{\pi (R E_{J_t})^2} \ln \frac{\bar{\xi}^2_{J_u} \bar{\xi}^2_{J_d}}{4(\bar{\xi}_{J_u} \cdot \bar{\xi}_{J_d})^2} \left(\frac{1}{\epsilon} + \ln \frac{4\pi \mu_f^2 \bar{N}^2}{R^4 E^2_{J_t} e^{\gamma_E}} \right), \\
S^{(1)}_{u} &= \frac{\alpha_s C_F}{\pi (R E_{J_t})^2} \ln \frac{\bar{\xi}^2_{J_u}}{R^2} \left(\frac{1}{\epsilon} + \ln \frac{4\pi \mu_f^2 \bar{N}^2}{R^4 E^2_{J_t} e^{\gamma_E}} \right), \\
S^{(1)}_{d} &= \frac{\alpha_s C_F}{\pi (R E_{J_t})^2} \ln \frac{R^2 \bar{\xi}^2_{J_d}}{4(\bar{\xi}_{J_u} \cdot \bar{\xi}_{J_d})^2} \left(\frac{1}{\epsilon} + \ln \frac{4\pi \mu_f^2 \bar{N}^2}{R^4 E^2_{J_t} e^{\gamma_E}} \right).
\end{aligned} \tag{A4}$$

The thin down jet with the cone radius r has a low invariant mass, whose dependence can be dropped in all other subprocesses of the factorization formula. This mass can then be integrated out trivially, and a thin subjet contributes an overall normalization to the factorization formula. Hence, the condition $4(\bar{\xi}_{J_d} \cdot \xi_{J_d})^2 / \xi^2_{J_d} = r^2$ required by the resummation formalism [47] is relaxed, and the Wilson line direction ξ_{J_d} can be arbitrary in principle. We utilize this freedom, choosing ξ_{J_d} to give the logarithmic coefficient of $S^{(1)}_d$ in Eq. (A4). This choice is feasible, because of $(\bar{\xi}_{J_u} \cdot \bar{\xi}_{J_d})^2 \sim (m_W / E_{J_t})^4 \sim O(r^2)$ in the considered kinematic region. The subtracted soft correction $S^{(1)}_{ud} - S^{(1)}_u - S^{(1)}_d$ is then negligible.

Next we discuss the soft gluons exchanged between the W-boson jet and the Wilson line of the top jet. Those between the fat subjet and the Wilson line of the top jet, and those between the thin subjet and the Wilson line yield

$$\begin{aligned}
S^{(1)}_{u\xi} &= \frac{\alpha_s C}{\pi (R E_{J_t})^2} \ln \frac{\bar{\xi}^2_{J_u} \xi^2_{J_t}}{4(\bar{\xi}_{J_u} \cdot \xi_{J_t})^2} \left(\frac{1}{\epsilon} + \ln \frac{4\pi \mu_f^2 \bar{N}^2}{R^4 E^2_{J_t} e^{\gamma_E}} \right), \\
S^{(1)}_{d\xi} &= -\frac{\alpha_s C}{\pi (R E_{J_t})^2} \ln \frac{\bar{\xi}^2_{J_d} \xi^2_{J_t}}{4(\bar{\xi}_{J_d} \cdot \xi_{J_t})^2} \left(\frac{1}{\epsilon} + \ln \frac{4\pi \mu_f^2 \bar{N}^2}{R^4 E^2_{J_t} e^{\gamma_E}} \right),
\end{aligned} \tag{A5}$$

respectively. The coefficient C differs from C_F, because a light quark in the W-boson jet and the Wilson line of the top jet are in separated color flows. Its explicit value is not crucial here. The minus sign in $S^{(1)}_{d\xi}$ arises, since the down quark is an anti-quark. It is straightforward to show, for the same collinear regulators $\bar{\xi}^2_{J_u} = \bar{\xi}^2_{J_d}$, that the combination $S^{(1)}_{u\xi} + S^{(1)}_{d\xi}$ is proportional to the polar angles θ_{J_u} and θ_{J_d}, which are power-suppressed in an

energetic top jet as indicated in Eq. (26) and by the perpendicular momentum conservation $E_{J_u}\theta_{J_u} = E_{J_{\bar{d}}}\theta_{J_{\bar{d}}}$. This observation realizes the postulation in the Introduction that soft gluon exchanges between the color-singlet W-boson jet and other subprocesses are expected to be suppressed in the limit of high jet energy. This soft correction does not double count the leading-power collinear dynamics, so the collinear subtraction is not necessary.

At last, the soft gluons exchanged among the up, down, and bottom subjets are handled in the similar way. We have the one-loop soft corrections

$$\begin{aligned} S_{ub}^{(1)} &= \frac{\alpha_s C}{\pi (R E_{J_t})^2} \ln \frac{\bar{\xi}_{J_u}^2 \bar{\xi}_{J_b}^2}{4(\bar{\xi}_{J_u} \cdot \bar{\xi}_{J_b})^2} \left(\frac{1}{\epsilon} + \ln \frac{4\pi \mu_f^2 \bar{N}^2}{R^4 E_{J_t}^2 e^{\gamma_E}} \right), \\ S_{db}^{(1)} &= -\frac{\alpha_s C}{\pi (R E_{J_t})^2} \ln \frac{\bar{\xi}_{J_d}^2 \bar{\xi}_{J_b}^2}{4(\bar{\xi}_{J_d} \cdot \bar{\xi}_{J_b})^2} \left(\frac{1}{\epsilon} + \ln \frac{4\pi \mu_f^2 \bar{N}^2}{R^4 E_{J_t}^2 e^{\gamma_E}} \right), \end{aligned} \tag{A6}$$

whose combination $S_{ub}^{(1)} + S_{db}^{(1)}$ is also power-suppressed. We conclude that the soft gluons are factorized into the fat subjets in our construction at least at one-loop level, and expect that such a factorization scheme can be extended to all orders.

---

[1] W. Bernreuther, J. Phys. G **35**, 083001 (2008).

[2] F.-P. Schilling, Int. J. Mod. Phys. A **27**, 1230016 (2012).

[3] G. Perez, Phys. Scr. T **158** 014008 (2013).

[4] J. M. Campbell and R. Keith Ellis, J. Phys. G. **42**, 015005 (2015).

[5] K. Agashe, A. Belyaev, T.Krupovnickas, G. Perez, and J. Virzi, Phys. Rev. D **77** 015003 (2008).

[6] B. Lillie, L. Randall, and L.-T. Wang, JHEP **0709**, 074 (2007).

[7] M. Perelstein and A. Spray, JHEP **1109**, 008 (2011).

[8] T. Plehn, M. Spannowsky, M. Takeuchi, and D. Zerwas, JHEP **1010**, 078 (2010).

[9] J. Berger, M. Perelstein, M. Saelim, and A. Spray, arXiv.1111.6594.

[10] A. Azatov, M. Salvarezza, M. Son, and M. Spannowsky, Phys. Rev. D **89**, 075001 (2014).

[11] T. Flacke, J. H, Kim, S. J. Lee, and S. H. Lim, JHEP **1405**, 123 (2014).

[12] M. Backovic, G. Perez, T. Flacke, and S. J. Lee, JHEP **1509**, 022 (2015).

[13] M. Backovic, T. Flacke, J. H. Kim and S. J. Lee, JHEP **1504**, 082 (2015).

[14] B. Gripaios, T. Mueller, M. A. Parker, and D. Sutherland, JHEP **1408**, 171 (2014).

[15] J, Reuter and M. Tonini, JHEP **1501**, 088 (2015).

[16] A. Ferroglia, B. D. Pecjak, and L. L. Yang, Phys. Rev. D **86**, 034010 (2012).

[17] A. Ferroglia, B. D. Pecjak, and L. L. Yang, JHEP **1210**, 180 (2012).

[18] B. Auerbach, S. V. Chkanov, and N. Kidonakis, arXiv:1301.5810.

[19] A. Ferroglia, S. Marzani, B. Pecjak, and L. L. Yang, JHEP **1401**, 028 (2014).

[20] B. Bhattacherjee, M. Guchait, S. Raychaudhuri, and K. Sridhar, Phys. Rev. D **82**, 055006 (2010).

[21] P. Bandyopadhyay and B. Bhattacherjee, Phys. Rev. D **84**, 035020 (2011).

[22] T. Plehn, M. Spannowsky, and M. Takeuchi, JHEP **1105**, 135 (2011).

[23] K. Blum *et al.*, Phys. Lett. B **702**, 364-369 (2011).

[24] M. Perelstein and A. Spray, JHEP **1109**, 008 (2011).

[25] B. Bhattacherjee, S. K. Mandal, and M. Nojiri, JHEP **1303**, 105 (2013).

[26] A. Chakraborty, D. K. Ghosh, D. Ghosh, and D. Sengupta, JHEP **1310**, 122 (2013).

[27] D. Duffty and Z. Sullivan, Phys. Rev. D **90**, 015031 (2014).

[28] A. Prasath, R. M. Godbole, S. D. Rindani, Eur. Phys. J. C **75**,9,402 (2015).

[29] J. Thaler and L.-T. Wang, JHEP **0807**, 092 (2008).

[30] D. E. Kaplan, K. Rehermann, M. D. Schwartz, and B. Tweedie, Phys. Rev. Lett. **101**, 142001 (2008).

[31] K. Rehermann and B. Tweedie, JHEP **1103**, 059 (2011).

[32] J. Thaler and K. V. Tiburg, JHEP **1202**, 093 (2012).

[33] C. Chen, Phys. Rev. D **87**, 074007 (2013).

[34] C. Chen, Phys. Rev. D **88**, 074009 (2013).

[35] S. Schätzel and M. Spannowsky, Phys. Rev. D **89**, 014007 (2014).

[36] M. Backovic, O. Gabizon, J. Juknevich, G. Perez, and Y. Soreq, JHEP **1402**, 176 (2014).

[37] A. J. Larkoski, F. Maltoni, M. Selvaggi, JHEP **1506**, 032 (2015).

[38] L. G. Almeida, M. Backovic, M. Cliche, S. J. Lee, M. Perelstein, JHEP **1507**, 086 (2015).

[39] J. A. Aguilar-Saavedra, B. Fuks, M. L. Mangano, Phys. Rev. D **91**, 094021 (2015).

[40] A. J. Larkoski, I. Moult, D. Neill, Phys. Rev. D **91**034035 (2015).

[41] J. Pilot, EPJ Web. Conf. **60**, 09003 (2013).

[42] S. Fleischmann, J. Phys. Conf. Ser. **452**, 012034 (2013).

[43] Y. Kitadono and H. n. Li, Phys. Rev. D **89**, No.11, 114002 (2014).

[44] D. Krohn, J. Shelton, and L.-T. Wang, JHEP **1007**, 041 (2010).

[45] B. Tweedie, Phys. Rev. D **90**, No.9, 094010 (2014).

[46] S. D. Ellis, Z. Kunszt, and D. Soper, Phys. Rev. Lett. **69**, 3615 (1992).

[47] H.-n. Li, Z. Li, and C. P. Yuan, Phys. Rev. Lett. **107**, 152001 (2011); Phys. Rev. D **87**, 074025 (2013).

[48] J. Isaacson, H.-n. Li, Z. Li, and C.-P. Yuan, arXiv:1505.06368.

[49] L. G. Almeida, S. J. Lee, G. Perez, I. Sung, and J. Virzi, Phys. Rev. D **79**, 074012 (2009).